Quantum Zeno Effect Rationalizes the Phonon Bottleneck in Semiconductor Quantum Dots

Svetlana V. Kilina, Amanda J. Neukirch, Bradley F. Habenicht, Dmitri S. Kilin, and Oleg V. Prezhdo

Phys. Rev. Lett. **110**, 180404 — Published 2 May 2013

DOI: 10.1103/PhysRevLett.110.180404

Quantum Zeno Effect Rationalizes the Phonon Bottleneck in Semiconductor Quantum Dots

Svetlana V. Kilina[1], Amanda J. Neukirch[2], Bradley F. Habenicht[3], Dmitri S. Kilin[4], and Oleg V. Prezhdo[5]

[1]*Department of Chemistry and Biochemistry, North Dakota State University, Fargo, North Dakota 58108, USA*

[2]*Department of Physics and Astronomy, University of Rochester, Rochester, New York 14627, USA*

[3]*Center for Nanophase Materials Science, Oak Ridge National Laboratory, Oak Ridge, Tennessee 37830, USA*

[4]*Department of Chemistry, University of South Dakota, Vermillion, South Dakota 57069, USA*

[5]*Department of Chemistry, University of Rochester, Rochester, New York 14627, USA*

Abstract

Quantum confinement can dramatically slow down electron-phonon relaxation in nanoclusters. Known as phonon-bottleneck, the effect remains elusive. Using a state-of-the-art time-domain ab initio approach, we model the observed bottleneck in CdSe and show that it occurs under quantum Zeno conditions. Decoherence in the electronic subsystem, induced by elastic electron-phonon scattering, should be significantly faster than inelastic scattering. Achieved with multi-phonon relaxation, the phonon-bottleneck is broken by Auger processes and structural defects, rationalizing experimental difficulties.

PACS numbers: 03.65.Xp, 03.65.Yz, 73.21.La, 78.67.Bf

Energy deposited during photoexcitation in traditional semiconductor materials is rapidly lost to lattice phonons. The ability to slow down phonon-assisted energy relaxation plays key roles in many applications ranging from optoelectronics and photovoltaics, to biology and medicine[1, 2]. Colloidal semiconductor quantum dots (QDs) are promising materials for the development of low cost, high efficiency devices, including lasers[3-5] fluorescent bio-tags[6, 7], quantum computers [8], light-emitting diodes [9], and solar cells [2, 5]. The discrete electronic transitions seen in the QD optical spectra [10] suggest a mismatch between the electronic and vibrational energy quanta, allowing for a dramatic decrease in the electron-phonon relaxation, known as the phonon bottleneck [2, 11]. Despite theoretical predictions [2], the majority of time-resolved experiments have shown picosecond relaxation, similar to that observed in bulk materials [12-14]. Moreover, the relaxation rates increase with decreasing QD size, despite the increasing electronic energy spacing [13-15]. The phonon-bottleneck has been observed only under very special conditions [16].

Several origins of the unexpectedly fast energy relaxation in QDs have been proposed. Auger-type processes break the bottleneck by allowing energy exchange between the excited electrons and holes, thereby opening up additional relaxation channels [17, 18]. Typically, holes form denser state manifolds and relax more quickly than electrons, and an Auger transfer of energy from the electron to the hole speeds up the relaxation. Further, QDs are not ideal structures. The underlying atomic structure, surface reconstruction and thermal fluctuations break electronic state degeneracies, creating complicated distributions of electronic states [19]. New non-radiative relaxation pathways result from surface impurities, defects, and passivating ligands, creating intermediate states with strong electron-vibrational couplings [12, 13, 20, 21]. Experimental realization of the phonon bottleneck is extremely difficult. As suggested by Kambhampati [13, 22], the bottleneck can be achieved by attenuation of the alternative relaxation channels. This idea was verified by Pandey and Guyot-Sionnest [16], who observed nanosecond relaxation of electrons from the $1P_e$ to $1S_e$ state, by synthesizing CdSe QDs with multiple layers of shells and ligands and separating electrons from holes.[16] Thick shells composed of multiple ZnS and ZnSe layers were needed to protect the QD core from a surface environment, to localize the electronic wavefunction inside the CdSe core, and to suppress the ligand-mediated relaxation channel [23, 24]. The authors also suggested that the shells trapped holes, decoupling them from core-bound electrons and suppressing Auger relaxation [25]. The

slowed relaxation allowed for hot electron extraction [23, 26] that constitutes an important mechanism for enhancing solar cell efficiencies [2, 27]. The difficulties in achieving the phonon-bottleneck in semiconductor QDs highlight the need for rigorous theoretical modeling of these systems.

The current letter reports time-domain density functional theory (TDDFT) calculations of the electron-phonon relaxation in CdSe QDs. In contrast to the traditional TDDFT calculations, which treat phonons classically, the present approach describes phonons semiclassically. The semiclassical description explicitly incorporates quantum decoherence effects within the electronic subsystem and shows, for the first time, that the phonon-bottleneck is directly related to the quantum Zeno effect. To achieve the bottleneck, elastic electron-phonon scattering inducing decoherence must be faster than the coherent electronic transition. The calculated electron-phonon relaxation time shows excellent agreement with the experimental data. The strong dependence of the relaxation time on the decoherence rate obtained by the ab initio time-domain simulation is rationalized analytically by a Fermi golden rule analysis. The suppression of the Auger processes is characterized by calculations on CdSe/ZnS core/shell QDs with and without defects. The atomistic study shows that the electron excited in the CdSe/ZnS system is contained within the core, while the hole is localized in the shell. This separation decouples the electron from the hole, preventing Auger recombination [17, 28]. Defects in the shell can destroy the electron-hole decoupling, allowing for fast relaxation. The established relationship between the phonon-bottleneck and the quantum Zeno effect, together with the atomistic details provided by the simulation, generate an understanding of the conditions necessary to achieve and control the phonon-bottleneck experimentally.

The vast majority of current theoretical and computational studies of semiconductor QDs focus on QD structure [29-32] and spectra [33-37]. Despite the availability of extensive experimental data on time-resolved excited state dynamics, [12-14, 38] time-domain simulations directly mimicking such experiments are rare [19, 39], largely due to the state-of-the-art methodologies needed for such simulations as well as the computational expense involved. Nonadiabatic molecular dynamics (NAMD) combined with TDDFT [19, 40] allows for ab initio modeling of non-equilibrium electron-phonon processes in nanoscale materials. The semiclassical treatment [41] of quantum decoherence effects is essential for accurate description of electronic transitions. Decoherence can be understood as a measurement of the state of the

electronic subsystem performed by the phonon environment. Also known as pure-dephasing, decoherence is caused by elastic electron-phonon scattering, which determines, for instance, luminescence linewidths of individual nanoparticles [42-44]. Fast decoherence, corresponding to frequent measurements of the quantum-mechanical state, inhibits transitions, leading to the quantum Zeno effect [45-50]. The reported simulations show explicitly that the phonon bottleneck is a manifestation of this phenomenon.

The optimized geometries of the $Cd_{33}Se_{33}$ and $Cd_{33}Se_{33}/Zn_{78}S_{78}$ core/shell QDs are shown in Figure 1. The black circles mark sulfur atoms removed from the ZnS shell to study the effect of shell defects on the electronic structure of the core/shell QDs. Each cluster was constructed using bulk wurzite lattice and relaxed to its lowest energy configuration at 0K. The geometry was optimized using DFT with a plane wave basis, as incorporated in the Vienna Ab initio Simulation Package (VASP) [51]. The Perdew and Wang (PW91) functional[52], paired with the Vanderbilt pseudopotentials [53], were used to account for electron exchange and correlation interactions. The simulations were performed in a periodically replicated cubic cell with at least 8A of vacuum between QD replicas. The electronic structure of the QDs in the optimal geometries was characterized further with the hybrid B3LYP functional incorporated into Gaussian 03 [54]. The CdSe QD was brought up to 300K by repeated velocity rescaling in VASP, and a 3 ps microcanonical MD trajectory was generated. 500 initial conditions were sampled from this trajectory to perform the NAMD-TDDFT simulations, as described in detail in [40, 55]. The vibrational and electronic degrees of freedom were evolved using 1fs and 1as time-steps, respectively.

The decoherence time was obtained with the optical response formalism [56], which allows one to use classical MD simulation. Decoherence of a quantum-mechanical superposition of two electronic states with the energy gap E is associated with fluctuations in the energy levels due to coupling to phonons. The pure-dephasing function is defined as

$$D(t) = \exp(i\omega t)\left\langle \exp\left(-\frac{i}{\hbar}\int_0^t \Delta E(\tau) d\tau \right) \right\rangle, \qquad (1)$$

where the angular bracket denotes canonical averaging, $\Delta E = E - \langle E \rangle$ is the deviation of the energy gap from its average value, and $\omega = \Delta E / \hbar$. The above expression can be approximated using the 2nd order cumulant expansion,

$$D(t) = e^{-g(t)},\ g(t) = \frac{1}{\hbar^2}\int_0^t d\tau_1 \int_0^{\tau_1} d\tau_2 \left\langle \Delta E(\tau)\Delta E(0)\right\rangle. \qquad (2)$$

Eq. (2) shows better numerical convergence than the direct expression (1), which involves averaging of an oscillating function. Both direct and cumulant methods have shown excellent agreement with experiment for several systems [42-44].

Following the experiment [16], we model the relaxation of the photoexcited electron from the $1P_e$ to $1S_e$ state of the CdSe QD. These states correspond to the 2nd and 1st lowest unoccupied molecular orbitals in the atomistic calculation, LUMO+1 and LUMO, top insert in Fig. 2a. The bottom insert in Fig. 2a shows the autocorrelation function of the energy gap between these states, $C(t) = \left\langle \Delta E(t)\Delta E(0)\right\rangle$, entering the cumulant function, Eq. (2). The initial value, $C(0) = \left\langle \Delta E^2(0)\right\rangle$, characterizes the fluctuation of the energy gap. The gap fluctuation is several meV and is much less than its absolute value of several hundred meV, because LUMO and LUMO+1 fluctuate in phase, top insert in Fig. 2a. The sub-100fs decay of the correlation function, $C(t)$, is typical of condensed phase systems [42-44, 48]. One can expect similar decay times in larger QDs, since on the one hand, the electron-phonon coupling decreases with system size leading to longer-lasting correlations, while on the other hand, LUMO and LUMO+1 will fluctuate less in phase, due to disorder and involvement of more phonons modes in larger systems. The direct and cumulant dephasing functions, shown in Fig. 1a, agree with each other and can be well fitted with a Gaussian with the characteristic pure-dephasing (decoherence) time of 36fs. This time is typical of other nanoscale systems [42-44].

Figure 2b shows the time-dependent population of the $1P_e$ state of the electron (LUMO+1) obtained using TDDFT-NAMD [40] with the semiclassical decoherence correction [41]. The population decay is due to the nonadiabatic, electron-phonon transition into the $1S_e$ state (LUMO). In addition to the calculated 36fs pure-dephasing time, 54=1.5x36 and 90=2.5x36 times are considered. Decreasing the coherence interval from 90 to 36fs increases the decay time. This phenomenon is indicative of the quantum Zeno effect [45-50]. In the limit of infinitely short coherence, the quantum transition stops. The calculated 670ps lifetime of the $1P_e$ state is in good agreement with the measured 1ns lifetime [16] The electron-phonon interaction and phonon-induced pure-dephasing can be modified through introduction of defects and ligands [21, 41], providing quantum control of the phonon-bottleneck.

Further understanding of the relationship between the phonon-bottleneck and the quantum Zeno effect is provided by the following analytic analysis based on the Fermi golden rule, describing the rate of transition between states 1 and 2:

$$k_{12} = \frac{2\pi}{\hbar} |V_{12}|^2 \sum_{\{f\}} \left|\langle i|f\rangle\right|^2 \delta\left(E_{1i} - E_{2f}\right). \quad (3)$$

Here, V_{12} is the non-adiabatic, phonon-induced coupling between electronic states 1 and 2. The Franck-Condon factor is determined by the overlap of the vibrational wave-functions, $\langle i|f\rangle$, associated with the initial and final electronic states. It is computed by summing over the set of final vibrational states, $\{f\}$, subject to equality of the initial, E_{1i}, and final, E_{2f}, electron-vibrational (vibronic) energy. Note that the Franck-Condon factor is closely related to the Huang-Rhys factor, e.g. see Eq. (19) of [57] and Eq. (V.9) of [58]. Represented in the energy-domain in terms of vibronic eigenstates, Eq. (3) can be recast in the time-domain, e.g. see Eq. (42) of [59]

$$k_{12} = \frac{1}{\hbar} |V_{12}|^2 \int \exp\left(i\Delta E_{12} t/\hbar\right) D(t) d(t/\hbar). \quad (4)$$

The time-domain representation of the Franck-Condon factor can be interpreted as a Fourier transform of the overlap of the vibrational wavepackets evolving in the two electronic states. The overlap gives the decoherence function [59]. The Fourier transform is evaluated at the electronic energy gap. Assuming that the decoherence function is Gaussian, $D(t) = \exp\left(-t^2/2{\tau_D}^2\right)$, Fig. 2a, one easily obtains an analytic expression for the transition rate, k_{12}, which depends on three parameters: the nonadiabatic coupling, V_{12}, the electronic energy gap, E_{12}, and the decoherence time, τ_D. Using order-of-magnitude values, $V_{12} = 10meV$ [60], $E_{12} = 0.1eV$, and $\tau_D = 30fs$, Fig. 2, one obtains the transition time, $1/k_{12} \sim 1ns$. The transition time shows Gaussian dependence on the electronic energy gap. Decreasing the gap to $E_{12} = 0.01eV$, characteristic of the quasi-continua of QD states at high excitation energies [19], shortens the transition time to $1/k_{12} \sim 50fs$. This simple analytic model supports the ab initio calculations and indicates that in order to achieve the phonon-bottleneck, one requires pure-dephasing times in the 10fs range and electronic energy gaps on the order of 0.1eV. Since the phonon frequencies of semiconductor QDs composed of heavy chemical elements are on the order $100cm^{-1}$~0.01eV, non-radiative

electronic transitions across 0.1eV energy gaps require multi-phonon processes, as suggested earlier [14, 38].

Elucidating the role of the shell in decoupling the electron from the hole and eliminating the Auger relaxation channel, Figure 3 shows the density of states (DOS) in the $Cd_{33}Se_{33}$ and $Cd_{33}Se_{33}/Zn_{78}S_{78}$ core/shell QDs. Recall, that the shell was essential in the experimental observation of the phonon bottleneck [16]. The DOS is higher for the valence band (VB) than the conduction band (CB), and the lowest energy hole states are closely spaced, in contrast to the electron states. Therefore, the Auger pathway indeed should accelerate the relaxation, breaking the phonon-bottleneck. The ZnS shell creates additional VB states near the band gap, but it does not affect the structure of the CB edge. The lowest energy states of the hole reside in the ZnS shell, while the electron remains inside the CdSe core, supporting the electron-hole separation concept. Removal of S atoms from the shell, representing shell defects, creates trap states close to the edge of the VB, Fig. 4a. The defects do not change the properties of the $1S_e$ state of the electron (LUMO), top row in Fig. 4b, but they do alter the localization of the lowest state of the hole (HOMO). In two of the three cases considered, S1 and S2, the HOMO is located the Zn dangling bond left by the missing S atom. These defect states are notably delocalized into the CdSe core: compare the HOMO of the perfect core/shell system in Fig. 3b with the HOMO of the S1 and S2 systems in Fig. 4b. The electron and hole are less isolated from each other in the presence of shell defects, opening up the Auger relaxation pathway[17] and rationalizing why imperfect shells lead to fast electron relaxation in the experiments [16].

In conclusion, the present work clearly shows that the phonon-bottleneck to the electron-phonon relaxation in semiconductor QDs is a special case of the quantum Zeno effect. Therefore, the conditions necessary for the quantum Zeno effect are also required for the phonon-bottleneck. In particular, the decoherence (pure-dephasing) time determined by elastic electron-phonon scattering should be significantly faster than the time-scale of the coherent electronic transition. The connection was illustrated by both explicit time-domain ab initio simulation and a Fermi golden rule analysis. The ab initio simulations showed good agreement with the experimental data. The simulations also indicated that the core/shell CdSe/ZnS structure used in the experiment indeed provides spatial separation of the electron and hole, which is essential for eliminating the Auger relaxation channel involving electron-hole energy exchange. Defects in the shell diminish the electron-hole separation, opening up the Auger channel. Introduction of

shells, dopants, defects and ligands can be used to alter the pure-dephasing rate, thereby providing quantum control over the conditions required for the quantum Zeno effect and the phonon-bottleneck.

The authors are grateful to Drs. Sergei Tretiak, Andrei Piryatinski, Heather Jaeger and Alexey Akimov for fruitful discussions, and to Levi Neukirch for comments on the manuscript. S. K. acknowledges support of the US Department of Energy Earlier Research Carrier Grant DE-SC008446 for financial support and the Center for Computationally Assisted Science and Technology (CCAST) at North Dakota State University and the Center for Integrated Nanotechnology (CINT) at Los Alamos National Laboratory for computer access and administrative support. OVP acknowledges support of the US Department of Energy grant no. DE-SC0006527.

Figure Captions

Figure 1. Optimized geometries of the CdSe and core-shell CdSe/ZnS clusters. The bottom and top rows show the (0001) and (0110), (1120) facets, respectively. Black circles mark 2- (S1) and 3-coordinated (S2, S3) surface sulfur atoms removed from the ZnS shell.

Figure 2. Electron-phonon dynamics in the $Cd_{33}Se_{33}$ QD. **(a)** Pure-dephasing function for the $1P_e$-$1S_e$ state pair, represented by LUMO+1 and LUMO, obtained directly (black line with open circles), Eq. (1), and using second-order cumulant expansion (red line with filled circles), Eq. (2). The dashed red line gives Gaussian fit of the cumulant function. The top inset shows evolution of the electron and hole energy levels near the band-gap. The bottom insert presents the autocorrelation function, $C(t)$, for the $1P_e$-$1S_e$ energy gap. **(b)** Decay of the photoexcited $1P_e$ (LUMO+1) state population into the $1S_e$ state (LUMO) calculated for different dephasing times. The dashed lines show linear fits.

Figure 3. Electronic structure of the CdSe and core-shell CdSe/ZnS QDs. **(a)** The bold black and red lines show density of states (DOS) for $Cd_{33}Se_{33}$ and $Cd_{33}Se_{33}/Zn_{78}S_{78}$, respectively. Each vertical line corresponds to an electronic state of the CdSe/ZnS QD, and the line length identifies localization of the state on the CdSe core (grey lines) and the ZnS shell (magenta lines). **(b)** Densities of occupied and vacant molecular orbitals near the band-gap.

Figure 4. Electronic structure of the CdSe/ZnS QD with missing S atoms. **(a)** The DOS shown in Figure 3a (solid lines) are superimposed with the DOS of the CdSe/ZnS with defects (dashed lines). The inset illustrates the alignment of the conduction and valence bands (CB and VB) in the CdSe/ZnS core/shell QDs. **(b)** HOMO and LUMO densities for the CdSe/ZnS QD with one removed S atom. Black circles mark positions of the removed atom.

References

[1] D. Kovalev, E. Gross, N. Künzner, F. Koch, V. Y. Timoshenko, and M. Fujii, Physical Review Letters **89**, 137401 (2002).

[2] A. Nozik, Annual review of physical chemistry **52**, 193 (2001).

[3] S. Strauf, K. Hennessy, M. T. Rakher, Y. S. Choi, A. Badolato, L. C. Andreani, E. L. Hu, P. M. Petroff, and D. Bouwmeester, Physical Review Letters **96**, 127404 (2006).

[4] V. I. Klimov, S. A. Ivanov, J. Nanda, M. Achermann, I. Bezel, J. A. McGuire, and A. Piryatinski, Nature **447**, 441 (2007).

[5] P. Kambhampati, Accounts of Chemical Research **44**, 1 (2011).

[6] M. Dahan, S. Lévi, C. Luccardini, P. Rostaing, B. Riveau, and A. Triller, Science **302**, 442 (2003).

[7] X. Michalet *et al.*, Science **307**, 538 (2005).

[8] J. Gorman, D. G. Hasko, and D. A. Williams, Physical Review Letters **95**, 090502 (2005).

[9] S. Coe, W. K. Woo, M. Bawendi, and V. Bulovic, Nature **420**, 800 (2002).

[10] G. D. Scholes and G. Rumbles, Nature materials **5**, 683 (2006).

[11] P. Kambhampati, Journal of Physical Chemistry C **115**, 22089 (2011).

[12] V. I. Klimov, A. A. Mikhailovsky, S. Xu, A. Malko, J. A. Hollingsworth, C. A. Leatherdale, H.-J. Eisler, and M. G. Bawendi, Science **290**, 314 (2000).

[13] R. R. Cooney, S. L. Sewall, K. E. H. Anderson, E. A. Dias, and P. Kambhampati, Physical Review Letters **98**, 177403 (2007).

[14] R. D. Schaller and V. I. Klimov, Physical Review Letters **96**, 97402 (2006).

[15] J. M. Harbold, H. Du, T. D. Krauss, K.-S. Cho, C. B. Murray, and F. W. Wise, Physical Review B **72**, 195312 (2005).

[16] A. Pandey and P. Guyot-Sionnest, Science **322**, 929 (2008).

[17] A. L. Efros, V. Kharchenko, and M. Rosen, Solid state communications **93**, 281 (1995).

[18] E. Hendry, M. Koeberg, F. Wang, H. Zhang, C. de Mello Donegá, D. Vanmaekelbergh, and M. Bonn, Physical Review Letters **96**, 57408 (2006).

[19] S. V. Kilina, D. S. Kilin, and O. V. Prezhdo, Acs Nano **3**, 93 (2008).

[20] P. Guyot-Sionnest, B. Wehrenberg, and D. Yu, The Journal of chemical physics **123**, 074709 (2005).

[21] S. Kilina, K. A. Velizhanin, S. Ivanov, O. V. Prezhdo, and S. Tretiak, Acs Nano (2012).

[22] R. R. Cooney, S. L. Sewall, E. A. Dias, D. M. Sagar, K. E. H. Anderson, and P. Kambhampati, Physical Review B **75** (2007).

[23] A. Pandey and P. Guyot-Sionnest, The Journal of Physical Chemistry Letters **1**, 45 (2009).

[24] Y. Chen, J. Vela, H. Htoon, J. L. Casson, D. J. Werder, D. A. Bussian, V. I. Klimov, and J. A. Hollingsworth, Journal of the American Chemical Society **130**, 5026 (2008).

[25] F. García-Santamaría, Y. Chen, J. Vela, R. D. Schaller, J. A. Hollingsworth, and V. I. Klimov, Nano Letters **9**, 3482 (2009).

[26] W. L. Chan, M. Ligges, A. Jailaubekov, L. Kaake, L. Miaja-Avila, and X. Y. Zhu, Science **334**, 1541 (2011).

[27] M. C. Beard, J. M. Luther, O. E. Semonin, and A. J. Nozik, Accounts of Chemical Research (2012).

[28] L. W. Wang, M. Califano, A. Zunger, and A. Franceschetti, Physical Review Letters **91**, 56404 (2003).

[29] A. Puzder, A. Williamson, F. Gygi, and G. Galli, Physical Review Letters **92**, 217401 (2004).

[30] J. Y. Rempel, L. Bernhardt, M. G. Bawendi, and K. F. Jensen, The Journal of Physical Chemistry B **110**, 18007 (2006).

[31] A. Alkauskas, P. Broqvist, and A. Pasquarello, Physical Review Letters **101**, 46405 (2008).

[32] P. Yang, S. Tretiak, A. E. Masunov, and S. Ivanov, The Journal of chemical physics **129**, 074709 (2008).
[33] Y. Semenov and K. Kim, Physical Review Letters **92**, 26601 (2004).
[34] E. Muljarov, T. Takagahara, and R. Zimmermann, Physical Review Letters **95**, 177405 (2005).
[35] H. Kamisaka, S. V. Kilina, K. Yamashita, and O. V. Prezhdo, Nano Letters **6**, 2295 (2006).
[36] A. Franceschetti, J. Luo, J. An, and A. Zunger, Physical Review B **79**, 241311 (2009).
[37] C. M. Isborn, S. V. Kilina, X. Li, and O. V. Prezhdo, The Journal of Physical Chemistry C **112**, 18291 (2008).
[38] R. D. Schaller, J. M. Pietryga, S. V. Goupalov, M. A. Petruska, S. A. Ivanov, and V. I. Klimov, Physical Review Letters **95**, 196401 (2005).
[39] Z. Guo, W. Z. Liang, Y. Zhao, and G. H. Chen, The Journal of Physical Chemistry C **112**, 16655 (2008).
[40] C. F. Craig, W. R. Duncan, and O. V. Prezhdo, Physical Review Letters **95**, 163001 (2005).
[41] B. F. Habenicht and O. V. Prezhdo, Physical Review Letters **100**, 197402 (2008).
[42] B. F. Habenicht, H. Karnisaka, K. Yarnashita, and O. V. Prezhdo, Nano Letters **7**, 3260 (2007).
[43] A. B. Madrid, K. Hyeon-Deuk, B. F. Habenicht, and O. V. Prezhdo, Acs Nano **3**, 2487 (2009).
[44] Z. Y. Guo, B. F. Habenicht, W. Z. Liang, and O. V. Prezhdo, Physical Review B **81**, 125415 (2010).
[45] O. V. Prezhdo, Physical Review Letters **85**, 4413 (2000).
[46] M. Simonius, Physical Review Letters **40**, 980 (1978).
[47] A. Bray and M. Moore, Physical Review Letters **49**, 1545 (1982).
[48] O. V. Prezhdo and P. J. Rossky, Physical Review Letters **81**, 5294 (1998).
[49] E. W. Streed, J. Mun, M. Boyd, G. K. Campbell, P. Medley, W. Ketterle, and D. E. Pritchard, Physical Review Letters **97**, 260402 (2006).
[50] S. Maniscalco, J. Piilo, and K. A. Suominen, Physical Review Letters **97**, 130402 (2006).
[51] G. Kresse and J. Furthmüller, Physical Review B **54**, 11169 (1996).
[52] J. Perdew, Phys. Rev. B **45**, 244 (1991).
[53] D. Vanderbilt, Physical Review B **41**, 7892 (1990).
[54] M. J. Frisch *et al.*, Gaussian 03, Revision C.02, 2003.
[55] O. V. Prezhdo, W. R. Duncan, and V. V. Prezhdo, Progress in Surface Science **84**, 30 (2009).
[56] S. Mukamel, *Principles of Nonlinear Optical Spectroscopy, edited by M. Lapp, J.-I. Nishizawa, BB Snavely, H. Stark, AC Tam, and T. Wilson* (Oxford University Press, New York, 1995).
[57] R. A. Marcus and N. Sutin, Biochimica et Biophysica Acta **811**, 265 (1985).
[58] P. F. Barbara, T. J. Meyer, and M. A. Ratner, J. Phys. Chem. **100**, 13148 (1996).
[59] O. V. Prezhdo and P. J. Rossky, The Journal of chemical physics **107**, 5863 (1997).
[60] S. V. Kilina, D. S. Kilin, V. V. Prezhdo, and O. V. Prezhdo, The Journal of Physical Chemistry C **115**, 21641 (2011).

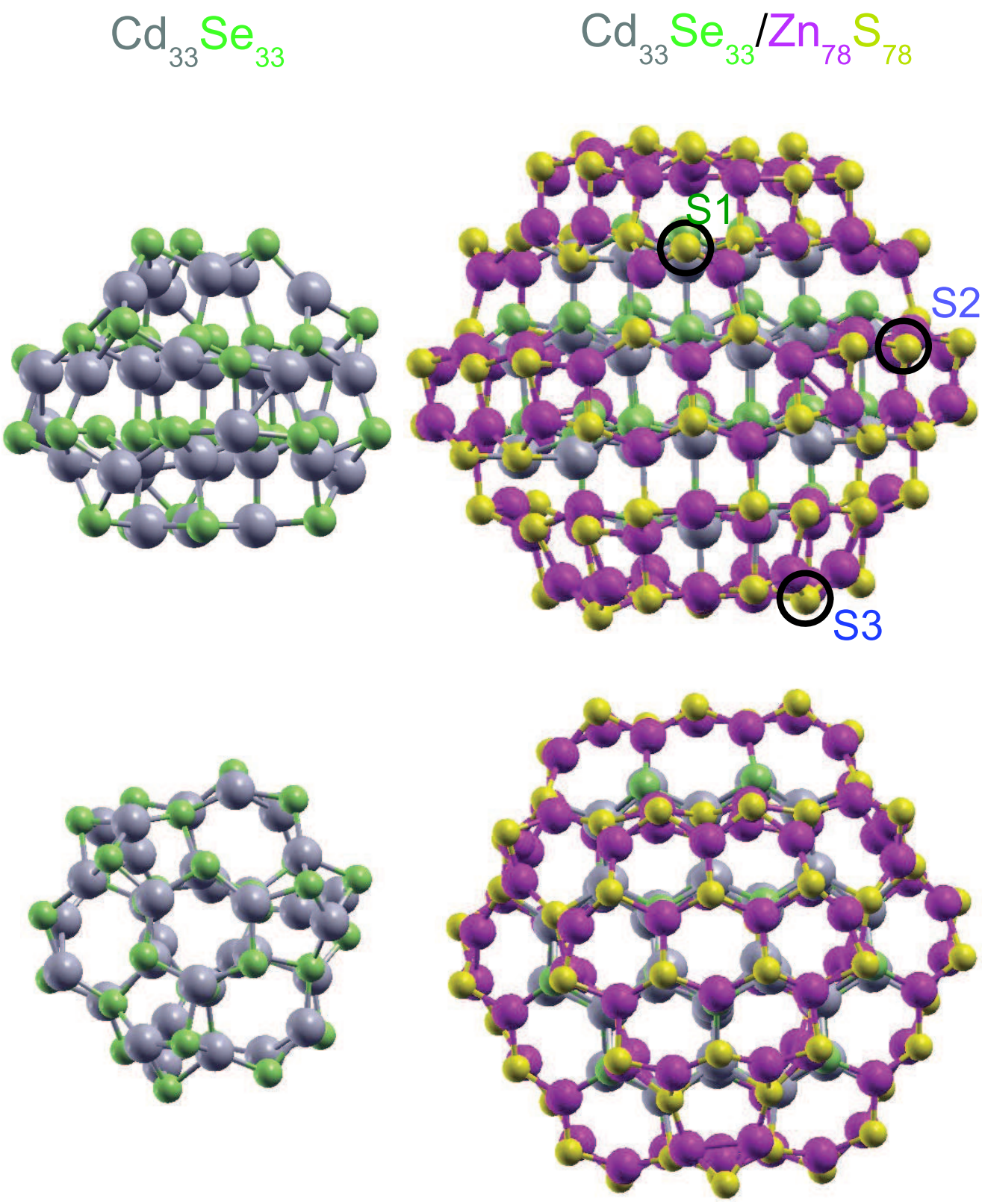

Figure 1 LZ13027 27MAR2013

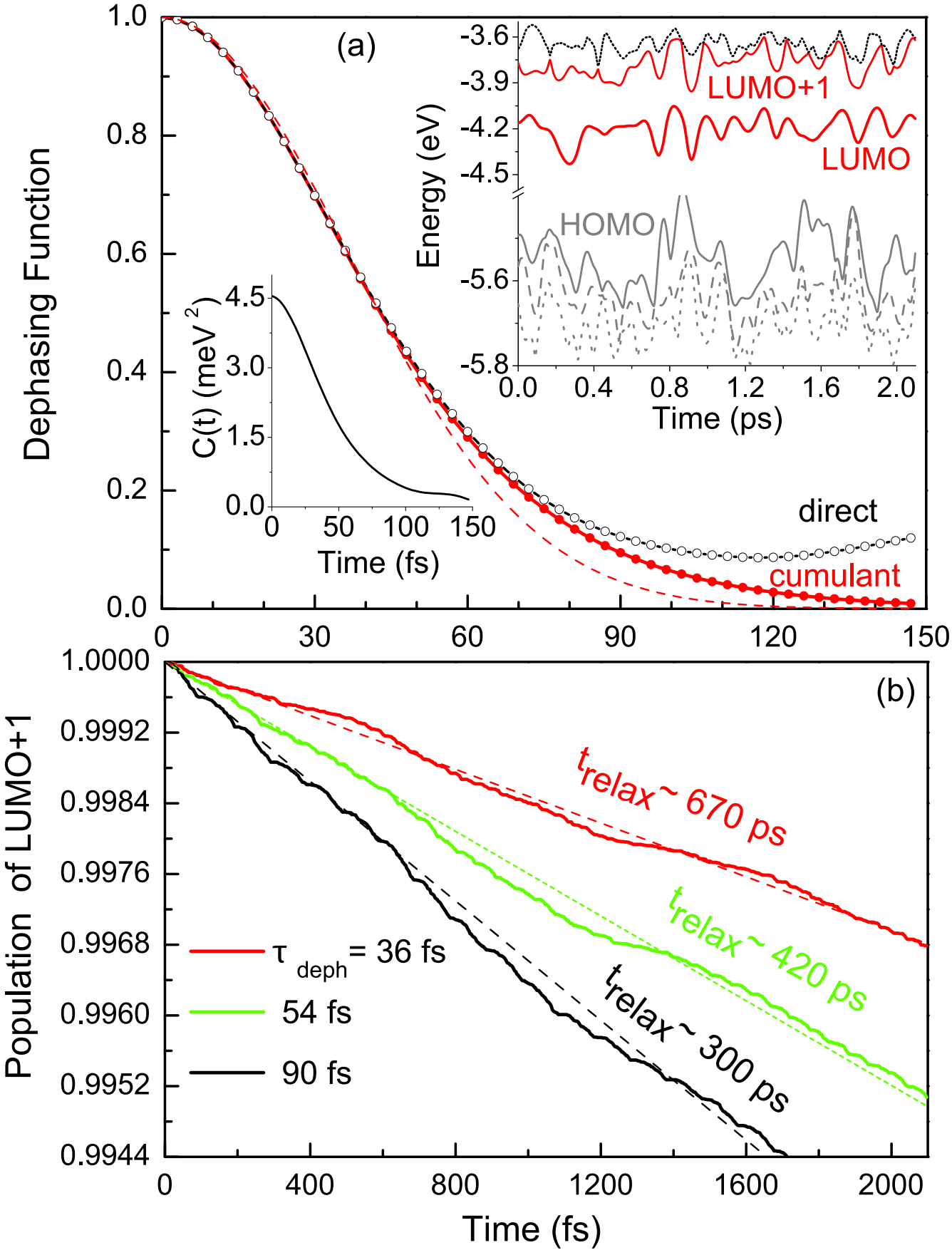

Figure 2 LZ13027 27MAR2013

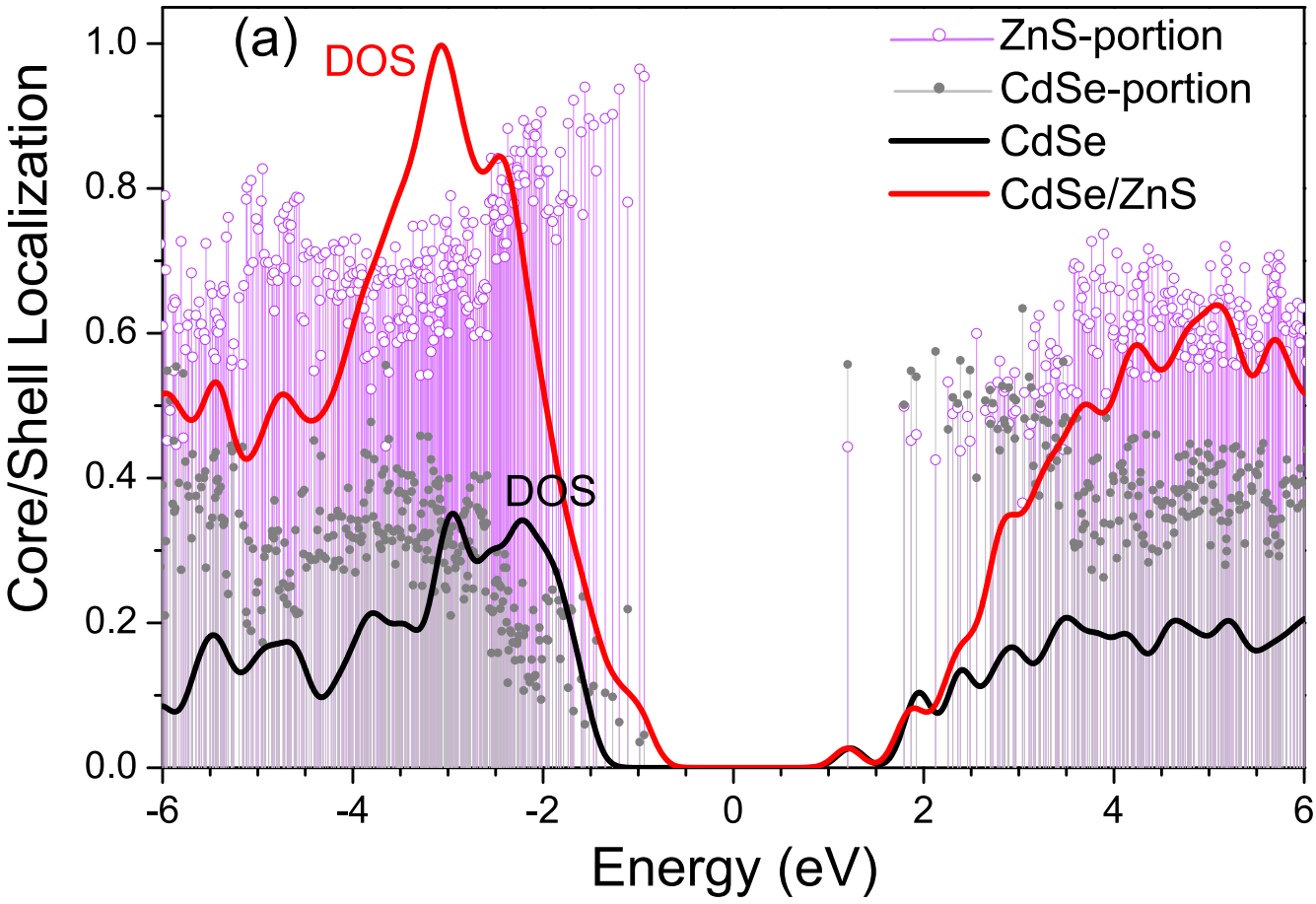

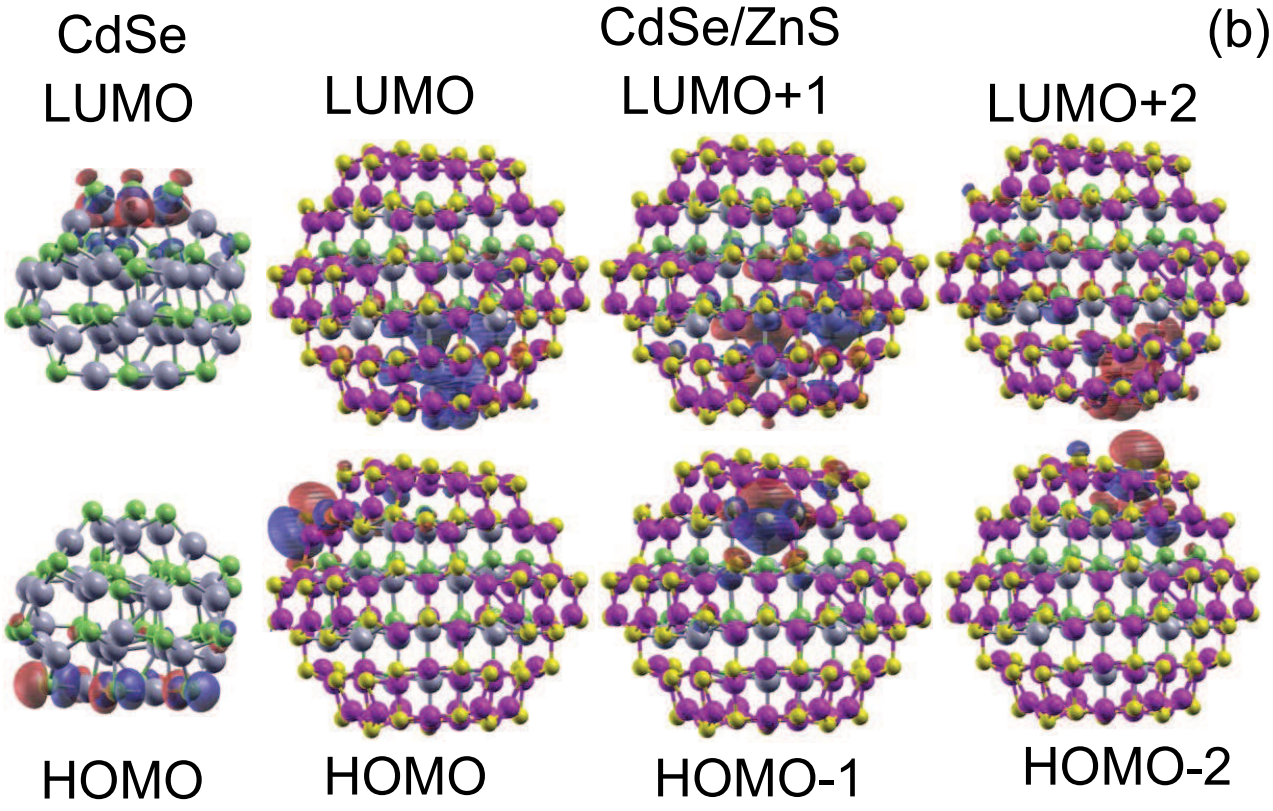

Figure 3 LZ13027 27MAR2013

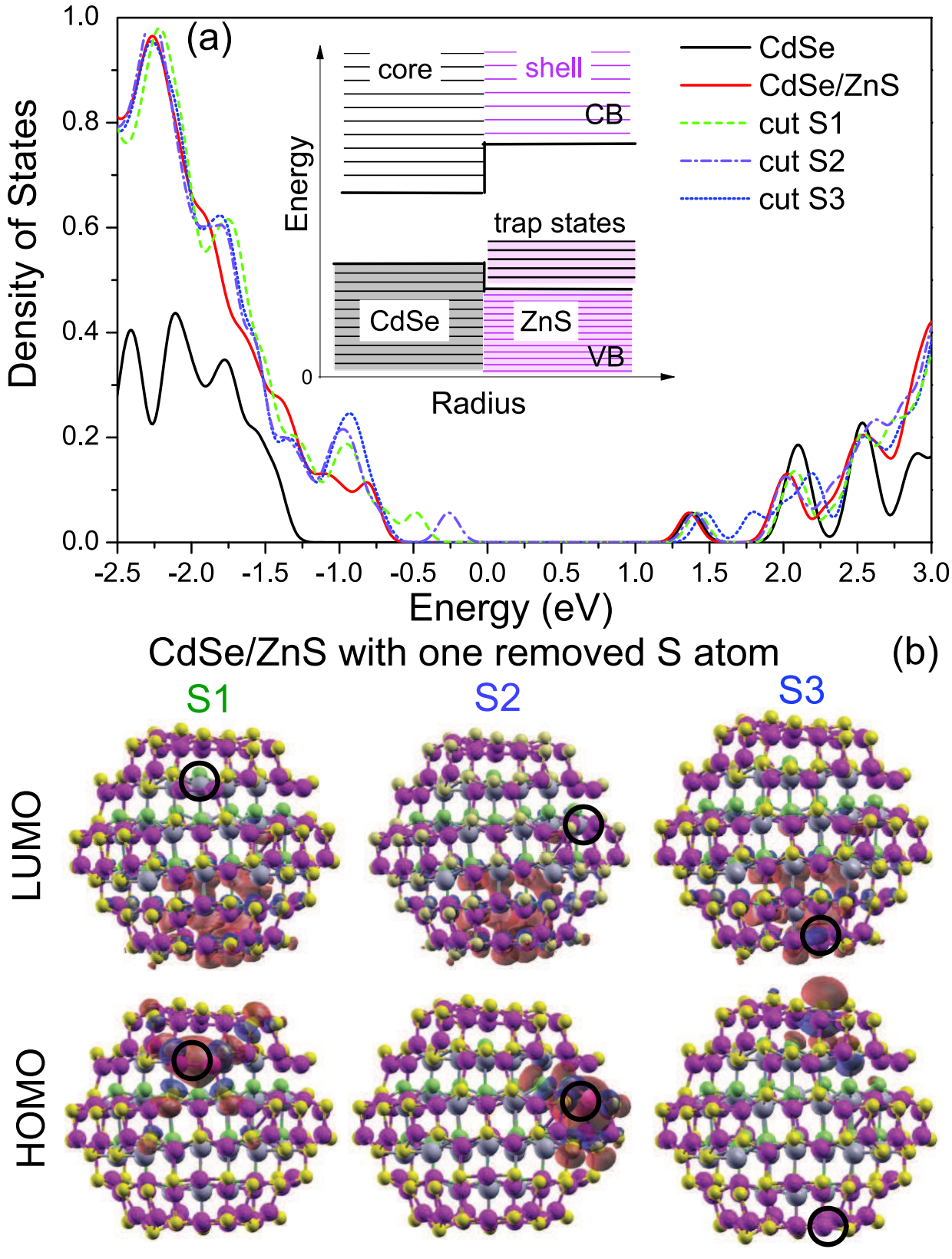

Figure 4 LZ13027 27MAR2013